Drift–diffusion kinetics of a confined colloid

2010 J. Phys.: Condens. Matter 22 195104

(http://iopscience.iop.org/0953-8984/22/19/195104)

J. Phys.: Condens. Matter **22** (2010) 195104 (7pp) doi:10.1088/0953-8984/22/19/195104

Drift–diffusion kinetics of a confined colloid

Yves Leroyer and Alois Würger

CPMOH, Université Bordeaux 1 & CNRS, 351 cours de la Libration, F-33405 Talence, France

Received 19 February 2010, in final form 16 March 2010
Published 16 April 2010
Online at stacks.iop.org/JPhysCM/22/195104

Abstract
The drift–diffusion equation on a finite interval with reflecting boundary conditions is solved by Laplace transformation. The Green function is obtained as a series in powers of $e^{-hu/D}$, where u is the drift velocity, D the diffusion coefficient and h the width of the interval. In the drift-dominated regime $hu/D \gg 1$, the first terms provide an exact solution in the limit of short and long times, and a good approximation in the intermediate regime. As a possible application, we discuss confined colloidal suspensions subjected to an external field.

1. Introduction

Drift–diffusion models describe stochastic processes with accumulation and noise terms [1]. The simplest case corresponds to a Fokker–Planck equation with constant drift velocity and diffusion coefficient [2], with applications ranging from decision tasks in cognitive science [3] to the evolution of droplet size distributions in turbulent clouds [4]. More complex variants deal with the effects of confinement on Brownian motion with a spatially varying mobility, or study how a discontinuous diffusion coefficient or drift velocity affect the mean first-passage time [5–7].

In colloid science, the interplay of drift and diffusion determines both the transient and stationary states of a suspension confined in a thin film or in a microchannel subject to an external field. Colloidal transport is of great interest for microfluidic devices and their applications [8, 9]. Fractionation or active mixing in complex fluids require external forces acting on the suspended particles or macromolecules. Body forces such as gravity and optical tweezers vary with the volume and thus are less efficient for small solutes, whereas the transport velocity due to interfacial forces is independent of the particle size. If electric fields are widely used in applications [10–13], in recent years thermal and chemical gradients have been shown to provide an alternative tool for manipulating colloidal suspensions on the microscale.

The kinetics of separation and mixing arise from the competition of Brownian motion and the forces acting on the suspended particles or macromolecules. With the Einstein coefficient $D \sim \mu m^2\ s^{-1}$, one finds that diffusive transport on the length scale of a microchamber is much slower than $1\ \mu m\ s^{-1}$. Thermal and chemical gradients may result in velocities of several $\mu m\ s^{-1}$ and thus provide an efficient means for moving particles. For comparison, the electrophoretic velocity may attain millimeters per second [14].

A chemical gradient has been used for focusing or dispersing a colloidal suspension in a Ψ-shaped microfluidic device [15]. The lateral diffusion of the mobile ions gives rise to a non-uniform salinity n_0, which in turn drives the silica beads towards regions of higher electrolyte strength. With an appropriate choice for the electrolyte solution, this diffusiophoretic effect permits us to rapidly spread the suspension over the whole channel or, in contrast, to concentrate the colloidal particles in the center [15]. Thermally driven sedimentation of charged latex beads in a microchamber was shown to confine the colloid within a layer of a few microns at the lower boundary [16, 17], similar to electrophoretic deposition [18]. Colloidal particles, ionic micelles, proteins and DNA are equally sensitive to thermal forces [19]. A radial temperature gradient in a thin film has been used for enhancing the concentration of charged particles in a colloid–polymer mixture by more than two orders of magnitude [20].

In most of these situations, the steady-state probability distribution is readily obtained; yet the time evolution of a given initial state and its kinetics towards the stationary density are less obvious. In the present paper we study the kinetics of the probability distribution $n(x, t)$ for constant D and u. In section 2 we present the model and relevant experimental situations. In sections 3 and 4 we give the Green function in terms of an infinite series and deal with the special case of a constant initial density. Section 5 discusses particular aspects in view of applications to colloidal systems and compares our result with previous theoretical work.

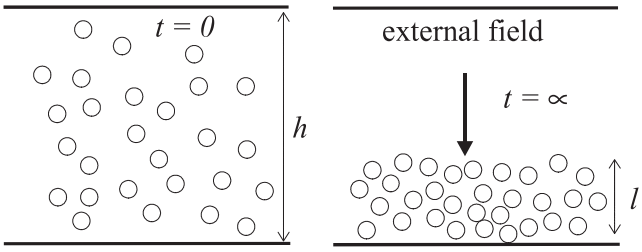

Figure 1. Schematic view of the constant density $n = n_0$ for zero field at $t = 0$, and of the stationary state $n = n_{\rm eq}$ after relaxation in an applied field.

2. Diffusion with drift in one dimension

The state of a colloidal suspension at time t is described by the density $n(x, t)$ where the coordinate is restricted to the interval $0 \leqslant x \leqslant h$. The particle current consists of two contributions:

$$J = un - D\frac{\mathrm{d}n}{\mathrm{d}x}, \tag{1}$$

where the first one describes the drift at speed u due to an external field and the second one accounts for diffusion with the Einstein coefficient D.

The steady-state distribution is obtained by solving $J(x) = 0$. Assuming D and u to be constant one finds the stationary particle density

$$n_{\rm eq}(x) = n_0 \frac{h}{\ell}\frac{\mathrm{e}^{-x/\ell}}{1 - \mathrm{e}^{-h/\ell}} \tag{2}$$

where the total number of particles is conserved. We have defined the average concentration

$$n_0 = \frac{1}{h}\int_0^h n(x, t)\,\mathrm{d}x,$$

and introduced the length scale

$$\ell = \frac{D}{|u|}$$

that gives the width of the steady-state distribution.

For micron-sized particles one has $D \sim \mu\mathrm{m}^2\,\mathrm{s}^{-1}$. Typical transport velocities are of the order of $u \sim \mu\mathrm{m}\,\mathrm{s}^{-1}$; such a value is attained, for example, for thermophoresis driven by a temperature difference of 20 K across a 100 μm wide channel. Thus one finds that the colloid will eventually concentrate in a layer of a few microns. Formally equation (2) is similar to sedimentation where the excess mass m of a particle gives rise to the buoyancy force mg.

The density and current satisfy the conservation equation

$$\frac{\partial J}{\partial x} + \frac{\partial n}{\partial t} = 0, \tag{3}$$

and the condition of zero current at the boundaries

$$J(0) = 0 = J(h). \tag{4}$$

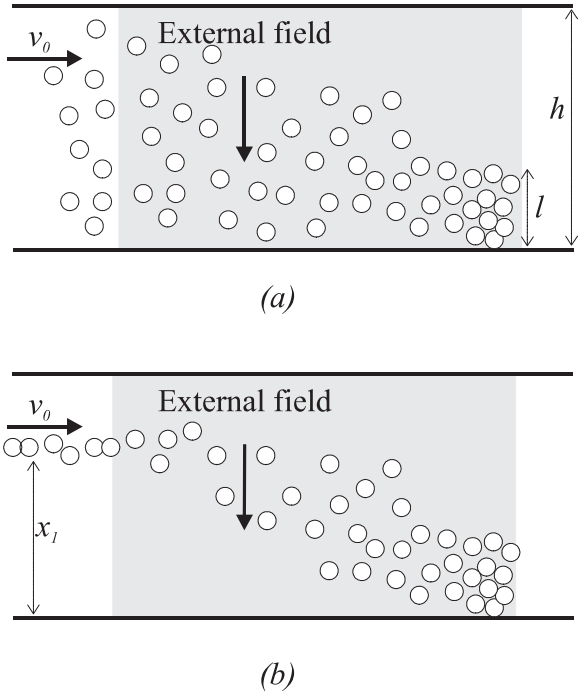

Figure 2. Schematic view of a microchannel of width h with ambient flow velocity v_0. In the gray zone an applied field perpendicular to the channel axis acts on the colloidal particles and thus enhances the concentration at the lower boundary. In the stationary state the colloidal distribution is characterized by a confinement length ℓ. (a) The initial density is uniform. (b) Same as (a) but with a localized beam of injected particles at $x = x_1$.

With the above definition of the current, one obtains the diffusion equation for the number density

$$\frac{\partial n}{\partial t} = D\frac{\partial^2 n}{\partial x^2} - u\frac{\partial n}{\partial x}, \tag{5}$$

and corresponding boundary conditions from (4).

Previous work on this drift–diffusion model has concentrated on the effective diffusion coefficient [2]. Here we consider the transport kinetics, that is, the time evolution of the number density n of colloidal particles and its relaxation towards the equilibrium distribution.

Before starting evaluation of the solution of (5), we discuss relevant experimental situations. The simplest one is shown in figure 1, a colloidal suspension in a thin film subject to a perpendicular field along the x axis. If the field is constant and if the initial distribution $n(x, t = 0)$ does not depend on the in-plane coordinates y and z, the one-dimensional equation (5) constitutes a complete description of the problem. Indeed, diffusion in the y–z plane does not affect the density distribution $n(x, t)$. The situation of figure 1 corresponds to the set-up of [16], where a temperature gradient is applied to a microchamber of 20 μm; in the steady state the suspended latex beads are confined to a layer of thickness $\ell \sim \mu$m.

In figures 2 we show a microchannel with ambient flow velocity; a transverse field along the x axis is applied in the gray region. These situations are approximately described by the 1D model, if one replaces the parabolic velocity profile

across the channel by a constant value v_0 and if the latter is significantly larger than the lateral drift velocity, $u \ll v_0$. With these assumptions, diffusion along the channel in the z direction is negligible; the y axis is of no relevance, and the transverse kinetics reduces to a one-dimensional problem. In the experiment of [15], the ratio u/v_0 is of the order of 10^{-3}; neglecting the lateral velocity profile is expected to affect only the details close to the lower boundary. The upstream colloidal density defines the initial distribution $n(x, 0)$: figure 2(a) corresponds to an initial constant density; this case is treated in section 4. The situation described in figure 2(b) corresponds to the Green function of the problem, which we derive in section 3.

3. The Green function

For the sake of notational convenience we introduce the dimensionless variables

$$\tau = t\frac{|u|}{\ell}, \qquad \xi = \frac{x}{\ell}, \qquad \xi_0 = \frac{h}{\ell}. \tag{6}$$

In term of these variables equation (5) becomes

$$\frac{\partial n}{\partial \tau} = \frac{\partial^2 n}{\partial \xi^2} + \frac{\partial n}{\partial \xi}; \tag{7}$$

where we suppose $u < 0$, i.e. the applied field drives the solute in the negative x direction towards the boundary at $x = 0$; the opposite case $u > 0$ is accounted for by defining $\xi = \xi_0 - x/\ell$.

The parameter ξ_0 can be expressed as

$$\xi_0 = \frac{h}{\ell} = \frac{|u|}{D/h}$$

which is the ratio of the advection velocity u to that of diffusion over the channel width D/h, and is known as the Péclet number for particle diffusion [21]. This point will be discussed in section 5.1.

In experiments the initial distribution of the colloidal particles may be homogeneous through the whole channel as in figure 2(a) or be finite in one part as realized in the experiment of [15]. In order to deal with the general case, we define the Green function of the process, $g(\xi, \xi_1; \tau)$, which is the probability for a particle located at position ξ_1 at time $\tau = 0$ to be at position ξ at time τ. This function allows us to describe the time evolution of the initial distribution $n(\xi, 0)$:

$$n(\xi, \tau) = \int_0^{\xi_0} g(\xi, \xi_1; \tau) n(\xi_1, 0)\, \mathrm{d}\xi_1. \tag{8}$$

Inserting (8) in the diffusion equation (7) one finds that the Green function satisfies the diffusion equation

$$\frac{\partial g}{\partial \tau} = \frac{\partial^2 g}{\partial \xi^2} + \frac{\partial g}{\partial \xi}; \tag{9}$$

with the initial condition

$$g(\xi, \xi_1; \tau = 0) = \delta(\xi - \xi_1). \tag{10}$$

The zero current condition (4) results in

$$\left[g + \frac{\partial g}{\partial \xi}\right]_{\xi=0} = 0 = \left[g + \frac{\partial g}{\partial \xi}\right]_{\xi=\xi_0}. \tag{11}$$

This boundary condition problem is solved after Laplace transformation. The detailed calculation is given in the appendix; here we quote the result:

$$\begin{aligned} g(\xi, \xi_1, \tau) = {} & \frac{\mathrm{e}^{-\xi}}{1 - \mathrm{e}^{-\xi_0}} \\ & + \mathrm{e}^{-\xi} \sum_{k=-\infty}^{\infty} \mathrm{e}^{-k\xi_0} E(2k\xi_0 + \xi_1 + \xi, \tau) \\ & + \mathrm{e}^{-(\xi-\xi_1)/2} \sum_{k=-\infty}^{\infty} \sum_{\pm} w(2k\xi_0 + \xi + \xi_1, \tau), \end{aligned} \tag{12}$$

where we have defined the functions

$$\begin{aligned} w(\xi, \tau) &= \frac{1}{2\sqrt{\pi\tau}} \mathrm{e}^{-\frac{\tau^2+\xi^2}{4\tau}}, \\ E(\xi, \tau) &= \frac{1}{2}\mathrm{erf}\left(\frac{\tau - \xi}{2\sqrt{\tau}}\right) - \frac{1}{2}. \end{aligned} \tag{13}$$

The Error function defined by $\mathrm{erf}(z) = \frac{2}{\sqrt{\pi}} \int_0^z \exp(-y^2)\, \mathrm{d}y$ is an odd function of z : $\mathrm{erf}(z) = -\mathrm{erf}(-z)$.

We briefly discuss the behavior at short and long times. For $\tau \ll 1$ the functions E are equal to -1 for $k \geqslant 0$ and zero for negative k; with $\sum_{k=0}^{\infty} \mathrm{e}^{-k\xi_0} = 1/(1 - \mathrm{e}^{-\xi_0})$ one finds that the corresponding series cancels the first term on the right-hand side of (12). The functions w in the remaining series are exponentially small, except for the second term at $k = 0$, that is $\mathrm{e}^{-(\xi-\xi_1)/2} w(\xi - \xi_1, \tau)$. As a consequence, at short times the Green function is given by

$$g\,(\xi, \xi_1, \tau) = \frac{1}{2\sqrt{\pi\tau}} \mathrm{e}^{-\frac{(\xi-\xi_1+\tau)^2}{4\tau}} \qquad (\tau \ll 1). \tag{14}$$

This form ceases to be valid as soon as its values at the boundaries $\xi = 0$ and ξ_0 become significant. Not surprisingly, in physical coordinates x and t we recover the free diffusion propagator, that is, a Gaussian of width $\sqrt{Dt}$ and a maximum position $x_1 + ut$ which moves at a constant drift velocity u. Furthermore we can check that the initial condition is satisfied: the limit $\lim_{\tau\to 0} g(\xi, \xi_1, \tau) = \delta(\xi - \xi_1)$ implies that the probability density at $\tau = 0$ is concentrated at ξ_1.

Now we turn to the long-time limit $\tau \gg \xi_0$. From the functions w and E it is clear that both series in (12) vanish; thus g tends towards the stationary probability distribution

$$g_{\mathrm{eq}}(\xi) = \frac{\mathrm{e}^{-\xi}}{1 - \mathrm{e}^{-\xi_0}} \tag{15}$$

and becomes independent of ξ_1 and τ. The first term on the right-hand side accounts for the stationary distribution, whereas the series describe the transient from the initial state.

Most experimental situations realize the case of strong confinement, where the sedimentation length ℓ is significantly smaller than the width h, that is, $\xi_0 \gg 1$. Because of the exponential decay of the functions E and w, then the series

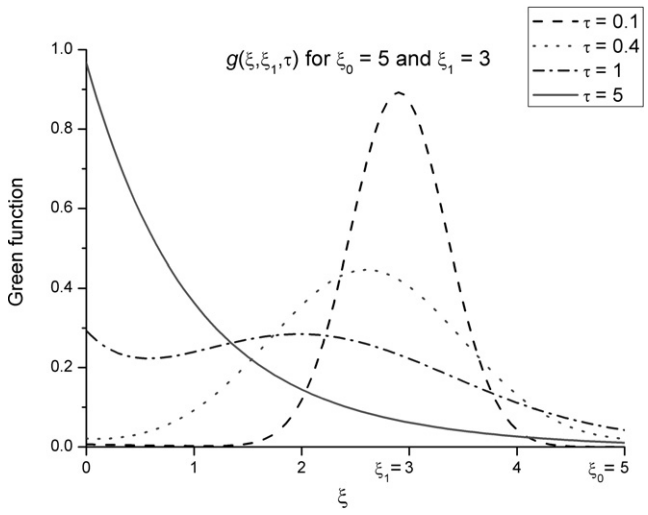

Figure 3. Variation of the reduced Green function $g(\xi, \xi_1, \tau)$ with the variable ξ at different times τ.

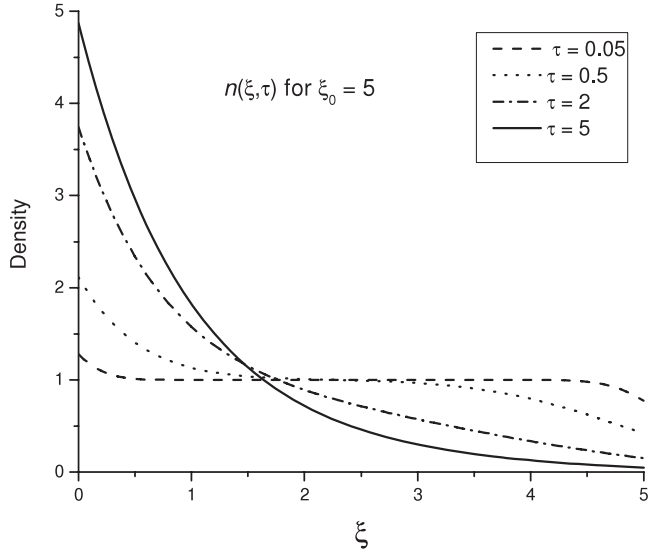

Figure 4. Time evolution of an initial flat density $n(\xi, 0) = n_0$. The curves show the density distribution at $\tau = 0.05, 0.5, 2, 5$.

in equation (12) can be truncated by discarding the terms for which the absolute value of the spatial argument of E and w is larger than ξ_0, resulting in

$$g(\xi, \xi_1, \tau) = \mathrm{e}^{-(\xi-\xi_1)/2}\{w(\xi_1 + \xi, \tau) + w(\xi - \xi_1, \tau) + w(2\xi_0 - \xi_1 - \xi, \tau)\} + \mathrm{e}^{-\xi}\{1 + E(\xi + \xi_1, \tau) + \mathrm{e}^{\xi_0}E(\xi + \xi_1 - 2\xi_0, \tau)\}. \quad (16)$$

This expression provides a very good approximation for $\xi_0 \geqslant 5$. It is plotted in figure 3 as a function of ξ for the width $\xi_0 = 5$ and initial position $\xi_1 = 3$ at the reduced times $\tau = 0.1; 0.4; 1; 5$.

At the shortest times the curves can hardly be distinguished from a Gaussian of width $\sqrt{\tau}$ and mean position $\xi_1 - \tau$ (see equation (14)). A more complex behavior occurs at $\tau \sim 1$: besides the maximum of the shifted initial distribution, the steady current towards the left gives rise to a second maximum at the lower boundary. At long times $\tau \gg \xi_0$ the probability distribution relaxes towards the steady state g_{eq}.

4. Constant initial distribution

The time-dependent probability distribution for an arbitrary initial condition is given by equation (8). Here we consider in more detail the particular case of a flat initial density $n(\xi_1, 0) = n_0$, where

$$n(\xi, \tau) = n_0 \int_0^{\xi_0} g(\xi, \xi_1; \tau)\, \mathrm{d}\xi_1.$$

The integration of the series of the Green function can easily be performed term by term. Starting from the expression of equation (12) we find after some algebra

$$n(\xi, \tau) = n_{\mathrm{eq}}(\xi) + n_0 \sum_{k=-\infty}^{\infty} \{\mathrm{e}^{-\xi/2}W(2k\xi_0 + \xi, \tau) - \mathrm{e}^{(\xi_0-\xi)/2}W[(2k+1)\xi_0 + \xi, \tau]\}$$

where we have defined the functions

$$W(\xi, \tau) = 2\tau w(\xi, \tau) + \mathrm{e}^{-\xi/2}(\tau - \xi + 1)E(\xi, \tau) + \mathrm{e}^{\xi/2}E(-\xi, \tau)$$

and the equilibrium value

$$n_{\mathrm{eq}}(\xi) = n_0\xi_0 \frac{\mathrm{e}^{-\xi}}{1 - \mathrm{e}^{-\xi_0}}. \quad (17)$$

For $\xi_0 \gg 1$ the density can be approximated to a good degree of accuracy by discarding in the sum the terms for which the absolute value of the spatial argument of W exceeds ξ_0:

$$n(\xi, \tau) = n_{\mathrm{eq}} + n_0\mathrm{e}^{-\xi/2}\{W(\xi, \tau) - \mathrm{e}^{\xi_0/2}W(\xi - \xi_0, \tau) - \mathrm{e}^{\xi_0/2}W(\xi + \xi_0, \tau)\}.$$

The last term contributes significantly only for large times. In figure 4 we plot $n(\xi, \tau)$ as a function of ξ for $\xi_0 = 5$ and the reduced times $\tau = 0.05, 0.5, 2, 5$. At short times $\tau \ll 1$ the external field carries the suspended particles at constant velocity u towards the left; the depression arising at the right appears as an excess density at the left boundary, whereas the inner part of the channel shows a plateau. As the reduced time τ becomes comparable to ξ_0, the depression and the bump extend through the channel; at longer times, they evolve towards the exponential distribution of the steady state (17). The latter is reached when the reduced time is of the order of the channel width, $\tau \sim \xi_0$.

5. Discussion

5.1. The Péclet number ξ_0

We have seen in section 3 that the parameter ξ_0

$$\xi_0 = \frac{h}{\ell} = \frac{|u|}{D/h}$$

is the Péclet number of the flow, defined as the ratio of the advection velocity u to that of diffusion over the channel width D/h. According to (2), efficient confinement requires a sedimentation length significantly smaller than the channel width, that is, a Péclet number much larger than unity, $\xi_0 \gg 1$.

We briefly discuss this condition in view of different driving mechanisms. For an aqueous suspension of micron-sized particles in a 100 μm wide channel, the diffusive velocity D/h is smaller than 10 nm s^{-1}. The drift velocity due to an applied electric field may attain millimeters per second, resulting in a very large Péclet number. A temperature gradient induces a thermo-osmotic flow along the particle surface; with $\nabla T \sim 0.1$ K μm^{-1} and the coefficient $D_T \sim 10$ μm^2 K s^{-1} [22, 23], the resulting transport velocity $u = -D_T \nabla T$ may attain several microns per second. The sedimentation length of micron-sized particles has been shown to be comparable to their diameter [16]. A non-uniform electrolyte gives rise to a drift velocity $u = D_{DP} \nabla n_0$ of several microns per second; in the experiment of [15] the salinity gradient ∇n_0 is not constant, thus giving rise to a more complex flow pattern than that studied in the present work. These estimates show that chemical and thermal gradients may be used for strong confinement with Péclet numbers of the order of 100.

5.2. Relevant timescales

Both the stationary state and the transient kinetics are determined by the competition between drift at velocity u and diffusion with the Einstein coefficient D. The corresponding timescales are given by the duration of driven transport across the channel width h:

$$t_T = \frac{h}{|u|}, \tag{18}$$

and by the diffusion time of a Brownian particle over a length h:

$$t_D = \frac{h^2}{D}. \tag{19}$$

These times are related by the coupling parameter ξ_0 according to $t_D = \xi_0 t_T$. For a weak external field ($\xi_0 < 1$) diffusion is faster and the probability distribution relaxes on a timescale t_D.

Here we are interested in the opposite case $\xi_0 > 1$. Then drift prevails and the stationary state is reached after a time t_T. We discuss the transient state in terms of the probability for a particle that started at $t = 0$ at the upper boundary $x = h$ to arrive at the lower boundary $x = 0$ after a time t; this probability is given by the Green function g. For large Péclet number, say $\xi_0 > 5$, it is sufficient to retain linear corrections in the small parameter $e^{-\xi_0}$ in the expression of g, equation (12), and the Green function is

$$g(0, \xi_0, \tau) = 1 + 4e^{\xi_0/2} w(\xi_0, \tau) + E(\xi_0, \tau) + e^{\xi_0} E(-\xi_0, \tau). \tag{20}$$

It turns out to be convenient to write the variable τ in the form $\tau = \xi_0 t/t_T$. In figure 5 we plot $g(0, \xi_0, \xi_0 t/t_T)$ as a function of the reduced time t/t_T for different values of the parameter ξ_0. Its time dependence at a given value for ξ_0 is best understood by a glance at figure 5. At short times $t \ll t_T$ the probability density is concentrated at $x = h$ or $\xi = \xi_0$, and it is very unlikely to find a particle at $x = 0$. In the long-time limit $t \gg t_T$ one reaches the asymptotic value $g_{eq} = 1/(1 - e^{-\xi_0})$ which is very close to unity. Figure 5 shows that in the reduced variable t/t_T the intermediate range becomes narrower with increasing ξ_0. The width of the cross-over region is readily obtained from equation (20): for large values of ξ_0 this function simplifies to $1 + E(\xi_0, \tau)$, or

$$g\left(0, \xi_0, \xi_0 \frac{t}{t_T}\right) = \frac{1}{2} + \frac{1}{2}\mathrm{erf}\left(\frac{t - t_T}{2\sqrt{t t_T}}\sqrt{\xi_0}\right) \qquad (\xi_0 \gg 1). \tag{21}$$

Thus the width of the cross-over region of figure 5 between the short-time and the long-time regimes, decreases with the inverse square root of the Péclet number:

$$\Delta t \sim \frac{t_T}{\sqrt{\xi_0}}. \tag{22}$$

In the limit $\xi_0 \to \infty$, the error function is given by the sign of its argument and the propagator tends towards a step function $g(0, \xi_0, \xi_0 t/t_T) \to \Theta(t - t_T)$. In this limit diffusion is completely overwhelmed by the drift process; Brownian motion is irrelevant on the timescale t_T, which is the duration of particle transport across the channel.

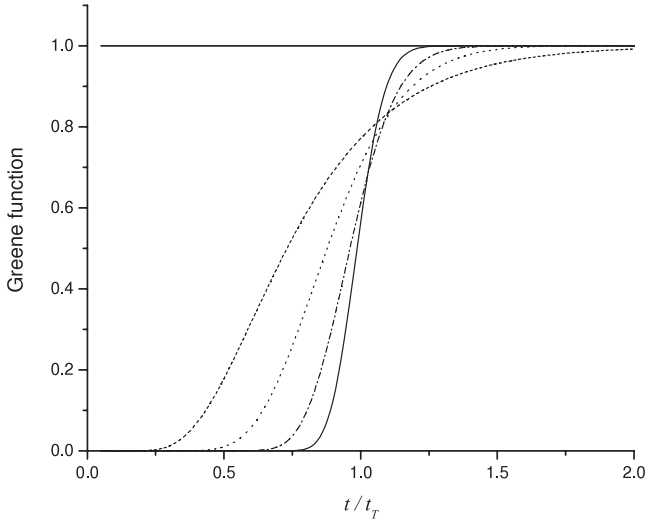

Figure 5. The Green function $g(0, \xi_0, \xi_0 t/t_T)$ which gives the probability for a particle starting at time $t = 0$ from the upper side of the channel ($\xi_1 = \xi_0$) to arrive at the opposite side ($\xi = 0$) at time t. This probability density is plotted as a function of time in units of t_T for different values of $\xi_0 = 10$ (dashed), 30 (dotted), 100 (dashed–dotted) and 300 (solid).

5.3. Hydrodynamic interactions

The present work relies on a single-particle picture which is valid at sufficiently low concentrations. Collective effects on transport coefficients comprise 'thermodynamic' and hydrodynamic contributions [24]. Thus collective diffusion in a semidilute colloidal suspension enhances the Einstein coefficient according to

$$D = D_0(1 + 2B\phi + 6.55\phi),$$

where ϕ is the volume fraction. The virial coefficient B is due to two-particle interactions; it is negative for attractive forces, whereas steric interactions and the corresponding excluded volume lead to a positive value of B. The second term with the numerical coefficient 6.55 describes the hydrodynamic drag exerted by a moving bead on the surrounding fluid [25]. Similar corrections of opposite sign occur for the gravity-driven sedimentation velocity. In contrast, motion driven by surface forces, such as electro-osmosis or thermo-osmosis in the particle's electric double layer, are hardly affected by hydrodynamic interactions. In a bulk colloid, the drift velocity u is independent of the volume fraction.

Additional effects occur close to the solid boundaries. The diffusion coefficient D shows a reduction linear in the inverse distance from the confining wall [21, 26]. The drift velocity u is reduced by a term that varies with the cube of the inverse distance from the wall [27]; thus boundary effects are significantly weaker than for the diffusion coefficient. In general, boundary effects are negligible as long as the film thickness is much larger than the bead size.

5.4. Comparison with an approach based on Fourier series

In a very recent paper, Zhang *et al* solved the drift–diffusion equation (9) by expanding the initial state in a Fourier series and separating the variables x and t [3]. Rewriting their equations (A4)–(A16) in our notation, we obtain the Green function in the form

$$g(\xi,\xi_1,\tau) = g_{\rm eq}(\xi) + \mathrm{e}^{-\xi/2}\sum_{n=1}^{\infty} g_n(\xi_1)\mathrm{e}^{-\lambda_n\tau} \times\left[\cos(q_n\xi) - \frac{\sin(q_n\xi)}{2q_n}\right], \tag{23}$$

with the wavevector and the relaxation rate

$$q_n = n\frac{\pi}{\xi_0}, \qquad \lambda_n = q_n^2 + \frac{1}{4}. \tag{24}$$

For the initial condition $g(\xi,\xi_1,0) = \delta(\xi-\xi_1)$ the coefficients $g_n(\xi_1)$ become

$$g_n(\xi_1) = \frac{2\mathrm{e}^{\xi_1/2}}{\xi_0\left(1+\frac{1}{4}q_n^{-2}\right)}\left[\cos(q_n\xi_1) - \frac{\sin(q_n\xi_1)}{2q_n}\right]. \tag{25}$$

We briefly discuss the convergence of this series expansion.

For large n the sine functions vanish in both (23) and (25). Thus the spatial part of each term is, up to a numerical prefactor, $\mathrm{e}^{-(\xi-\xi_1)/2}\cos(q_n\xi)\cos(q_n\xi_1)$. At $\tau = 0$ the series does not converge smoothly, as is well known for the Fourier representation of a delta peak $\delta(\xi-\xi_1)$. At finite times the exponential factor $\mathrm{e}^{-\lambda_n\tau}$ vanishes for large enough n; in order to obtain a good representation for $g(\xi,\xi_1,\tau)$, the sum over n has to be pushed well beyond $n^* = \tau^{-\frac{1}{2}}\xi_0/\pi$. Thus the Fourier series converges rapidly at long times and for small values of ξ_0; in the short-time limit, more and more terms have to be retained as τ decreases.

Our equation (12) gives the Green function as a series in powers of $\mathrm{e}^{-\xi_0}$ which converges smoothly for any τ and ξ. For short times $\tau \ll 1$ one recovers the exact expression (14); in the opposite limit $\tau \gg \xi_0$ the series disappears and leaves the steady-state distribution $g_{\rm eq}$. For a sufficiently strong drift term, say $\xi_0 > 5$, the few terms given in (16) provide a very good approximation in the intermediate range.

6. Summary

For the drift–diffusion model in a finite interval with constant coefficients, we have obtained an exact solution in terms of a series in powers of $e^{-\xi_0}$ where ξ_0 is the Péclet number. In drift-dominated applications ($\xi_0 \gg 1$), such as colloidal transport in confined geometries, the Green function of the diffusion equation is very well approximated by (16) in terms of a few elementary functions.

The characteristic time for transport at velocity u over the length h is, not surprisingly, given by $t_{\rm T}$ in (18). In the vicinity of $t \sim t_{\rm T}$ the Green function $g(0,\xi_0,\tau)$ increases from 0 to the steady-state value $1/(1-\mathrm{e}^{-\xi_0})$, as illustrated in figure 5. The duration Δt of this cross-over decreases with the Péclet number according to (22).

The drift–diffusion kinetics shown in figure 3, and in particular the two-peak structure at intermediate times, should be visible for confined colloidal suspensions subject to an external field.

Appendix

We solve the boundary value problem equations (9), (10) and (11) by Laplace transformation. Let $G(\xi,\xi_1,p) = \mathcal{L}_\tau\{g\}$ be the Laplace transform of $g(\xi,\xi_1,\tau)$; equations (9) and (10) lead to

$$pG - \partial_\xi^2 G - \partial_\xi G = \delta(\xi-\xi_1).$$

The general solution of this equation is

$$G(\xi,\xi_1,p) = A(p)\mathrm{e}^{-\frac{\delta+1}{2}\xi} + B(p)\mathrm{e}^{\frac{\delta-1}{2}\xi} + \frac{1}{\delta}\mathrm{e}^{-(\xi-\xi_1)/2}\,\mathrm{e}^{-\frac{\delta}{2}|\xi-\xi_1|} \tag{26}$$

where

$$\delta = \sqrt{1+4p}.$$

The boundary conditions (equation (11)) remain unchanged:

$$G + \left.\frac{\partial G}{\partial\xi}\right|_{\xi=0} = 0 = G + \left.\frac{\partial G}{\partial\xi}\right|_{\xi=\xi_0}.$$

From these equations we get for the functions $A(p)$ and $B(p)$:

$$A(p) = \frac{1}{\delta}\frac{\mathrm{e}^{\xi_1/2}}{1-\mathrm{e}^{-\delta\xi_0}}\left[\mathrm{e}^{-\frac{\delta}{2}(2\xi_0-\xi_1)} + \frac{\delta+1}{\delta-1}\mathrm{e}^{-\frac{\delta}{2}\xi_1}\right],$$

$$B(p) = \frac{1}{\delta}\frac{\mathrm{e}^{\xi_1/2}\mathrm{e}^{-\delta\xi_0}}{1-\mathrm{e}^{-\delta\xi_0}}\left[\mathrm{e}^{-\frac{\delta}{2}\xi_1} + \frac{\delta-1}{\delta+1}\mathrm{e}^{\frac{\delta}{2}\xi_1}\right].$$

Replacing in these expressions $\frac{1}{1-\mathrm{e}^{-\delta\xi_0}}$ by $\sum_{k=0}^{\infty}\mathrm{e}^{-k\delta\xi_0}$ we can express the solution $G(\xi,\xi_1,p)$ (equation (26)) as follows:

$$\begin{aligned}\mathrm{e}^{(\xi-\xi_1)/2}G(\xi,\xi_1,p) &= v(|\xi-\xi_1|)\\ &+ \sum_{k=0}^{\infty} v[(2k+2)\xi_0 - \xi_1 + \xi] + v(2k\xi_0+\xi_1+\xi)\\ &+ v[(2k+2)\xi_0 - \xi_1 - \xi] + v[(2k+2)\xi_0 + \xi_1 - \xi]\\ &+ v_+(2k\xi_0+\xi_1+\xi) + v_-[(2k+2)\xi_0 - \xi_1 - \xi]\end{aligned}$$

where

$$v(\xi, p) = \frac{e^{-\delta\xi/2}}{\delta}, \qquad v_\pm(\xi, p) = \frac{e^{-\delta\xi/2}}{2p}\left(\frac{1}{\delta} \pm 1\right).$$

The inverse Laplace transform is expressed in terms of

$$w(\xi, \tau) = \mathcal{L}^{-1}\{v(\xi, p)\}, \qquad w_\pm(\xi, \tau) = \mathcal{L}^{-1}\{v_\pm(\xi, p)\}$$

where

$$w(\xi, \tau) = \frac{1}{2\sqrt{\pi\tau}} e^{-\frac{\tau^2+\xi^2}{4\tau}}$$

has already been defined in (13) and

$$w_\pm(\xi, \tau) = \frac{1}{2} e^{\mp\xi/2}\left[\mathrm{erf}\left(\frac{\tau \mp \xi}{2\sqrt{\tau}}\right) \pm 1\right]$$

we get

$$\begin{aligned} g(\xi, \xi_1, \tau) = e^{-(\xi-\xi_1)/2} \sum_{k=0}^{\infty} \{ & w(2k\xi_0 - \xi_1 + \xi) \\ & + w(2k\xi_0 + \xi_1 + \xi) \\ & + w[(2k+2)\xi_0 - \xi_1 - \xi] + w[(2k+2)\xi_0 + \xi_1 - \xi] \\ & + w_+(2k\xi_0 + \xi_1 + \xi) + w_-[(2k+2)\xi_0 - \xi_1 - \xi]\}. \end{aligned}$$

It is easy to show that each term of order k in the series is bounded by $e^{-k\xi_0}$, thus ensuring a quick convergence for $\xi_0 \gg 1$.

This expression can be simplified by expressing $w_\pm$ by

$$E(\xi, \tau) = \frac{1}{2}\mathrm{erf}\left(\frac{\tau - \xi}{2\sqrt{\tau}}\right) - \frac{1}{2}$$

and by noticing that w is an even function of ξ:

$$\begin{aligned} g(\xi, \xi_1, \tau) = {} & \frac{e^{-\xi}}{1 - e^{-\xi_0}} + e^{-(\xi-\xi_1)/2} \\ & \times \sum_{k=-\infty}^{\infty} \{w(2k\xi_0 + \xi_1 + \xi) + w[2k\xi_0 + \xi - \xi_1]\} \\ & + e^{-\xi} \sum_{k=-\infty}^{\infty} e^{-k\xi_0} E(2k\xi_0 + \xi_1 + \xi, \tau). \end{aligned} \tag{27}$$

Since the functions w and E vanish at long times, the Green function tends towards the stationary state:

$$\lim_{\tau\to\infty} g(\xi, \xi_1, \tau) = g_{\mathrm{eq}}(\xi) = \frac{e^{-\xi}}{1 - e^{-\xi_0}}.$$

In the short-time limit we recover the initial condition for g. Noting that E tends towards a step function, $E(\xi, \tau) \to -\Theta(\xi)$ as $\tau \to 0$, and that $\lim_{\tau\to 0} w(\xi, \tau)$ vanishes for $\xi \neq 0$ and diverges at $\xi = 0$, one readily finds

$$\lim_{\tau\to 0} g(\xi, \xi_1, \tau) = \delta(\xi - \xi_1).$$

References

[1] Risken H 1989 *The Fokker–Planck Equation: Methods of Solutions and Applications* (Berlin: Springer)
[2] Khanta M and Balakrishnan V 1983 *J. Phys. C: Solid State Phys.* **16** 6291
[3] Zhang J, Bogacz R and Holmes P 2009 *J. Math. Psychol.* **53** 231
[4] McGraw R and Liu Y 2006 *Geophys. Res. Lett.* **33** 03802
[5] Morelli S, Santangelo R and Vincenzi S 1991 *Il Nuovo Cimento* C **14** 377
[6] Lançon P, Batrouni G, Lobry L and Ostrowsky N 2001 *Europhys. Lett.* **54** 28
[7] Bénichou O and Desbois J 2009 *J. Phys. A: Math. Gen.* **42** 015004
[8] Stone A, Stroock A D and Ajdari A 2004 *Annu. Rev. Fluid Mech.* **36** 381
[9] Squires T M and Quake S R 2005 *Rev. Mod. Phys.* **77** 977
[10] Viovy J L 2000 *Rev. Mod. Phys.* **72** 813
[11] Marcos, Yang C, Ooi K T, Wong T N and Masliyah J H 2004 *J. Colloid Interface Sci.* **275** 679
[12] Kline T R, Chen G and Walker S L 2008 *Langmuir* **24** 9381
[13] Anderson J L 1989 *Ann. Rev. Fluid Mech.* **21** 61
[14] Hiemenz P C and Rajagopalan R 1997 *Principles of Colloid and Surface Chemistry* (New York: Dekker)
[15] Abécassis B *et al* 2008 *Nat. Mater.* **7** 785
[16] Weinert F M and Braun D 2008 *Phys. Rev. Lett.* **101** 168301
[17] Di Leonardo R, Ianni F and Ruocco G 2009 *Langmuir* **25** 4247
[18] Böhmer M 1996 *Langmuir* **12** 5747
[19] Iacopini S, Rusconi R and Piazza R 2006 *Eur. Phys. J.* E **19** 59
[20] Jiang H-R *et al* 2009 *Phys. Rev. Lett.* **102** 208301
[21] Happel J and Brenner H 1991 *Low-Reynolds Number Hydrodynamics* (Dordrecht: Kluwer)
[22] Piazza R and Parola A 2008 *J. Phys.: Condens. Matter* **20** 153102
[23] Würger A 2008 *Phys. Rev. Lett.* **101** 108302
[24] Russel W B, Saville D A and Schowalter W R 1989 *Colloidal Dispersions* (Cambridge: Cambridge University Press)
[25] Batchelor G K 1972 *J. Fluid Mech.* **52** 245
[26] Brenner H 1961 *Chem. Eng. Sci.* **16** 242
[27] Keh H J and Anderson J L 1985 *J. Fluid Mech.* **153** 417